Proceedings World Geothermal Congress 2010
Bali, Indonesia, 25-29 April 2010

Contribution of Geophysical and Temperature Logs Data to Geothermal Exploration on the Gulf of Suez, Egypt

Mohamed Abdel Zaher[1], Mohamed El Nouby[2], Essam Ghamry[3], and Sachio Ehara[1]

[1.] Laboratory of Geothermic, Faculty of Engineering, Kyushu University, Japan; [2.] Egyptian Geological Survey and Mining Authority (EGSMA), Egypt; [3.] National Research Institute of Astronomy and Geophysics, Egypt

Keywords: geothermal resources, temperature logs, temperature gradient, heat flow, Bouguer anomaly map, aeromagnetic map

ABSTRACT

Egypt is located in the northeastern corner of the African continent and bounded to the east by Red Sea and what has been interpreted as a median spreading center in the Red Sea and Gulf of Suez which may reflect that these areas are the most promising for geothermal exploration. Temperature logs of about 105 marine oil wells were used for estimating the distribution of subsurface temperatures and the heat flows in Gulf of Suez region in order to demonstrate the geothermal resources in that area. Generally, highest temperature gradients were recorded southward and on rift margins and around the hot spring areas on the eastern margin of the Gulf of Suez. Simultaneously, High heat flows are recorded at the hot spring regions especially around Hammam Faraun hot spring. Analyses of Bouguer anomaly and aeromagnetic maps of the Gulf of Suez were used for delineating the subsurface structures and tectonic framework of the area. Integration between these maps and thermal logs elucidated the deep seated structure at the hottest areas. Thus, the thermal maturity lines on any cross section across the Gulf of Suez would be slightly concave and reflective of basement structure.

1. INTRODUCTION

Egypt is located in the northeastern corner of the African continent and bounded to the east by the Red Sea and what has been interpreted as a median spreading center in the Red Sea and Gulf of Suez (Mckenzie et al., 1970) which may reflect that this area is an important area for geothermal development. The far northern end of the Red Sea is divided into two parts by the Sinai Peninsula; Gulf of Suez in the west and Gulf of Aqaba in the east as shown in Fig. (1). The Gulf of Suez, an important shipping route for oil and other products, lies along the edges of the African country of Egypt and the Sinai Peninsula. It is approximately 314 km in length and 19 to 43 km in width and the water depth never exceeds 200 meters. Temperature logs of more than 100 marine oil wells were used for elucidating the subsurface temperature regime and heat flow on the Gulf of Suez region and compared with the analyses and processes of Bouguer anomaly and aeromagnetic maps of the Gulf of Suez. Also, geochemical interpretation was made for the thermal waters of the hot springs on the eastern and western sides of the Gulf of Suez.

2. GEOLOGICAL REGIN

The Red Sea occupies part of a large rift valley in the continental crust of Africa and Arabia. This break in the crust is part of a complex rift system that includes the East African Rift System (Said, 1962). The Red Sea bifurcates into the Gulfs of Suez and Aquaba, with the Sinai Peninsula in between. Gulf of Suez represents an elongated NW-SE trending trough extended more than 300 km in length and can be divided into three parts; the northern sector of the Gulf dips to SW, the central part dips to the NE, and the southern dips to the SW. The structure of the Gulf of Suez region is governed by normal faults and tilted blocks whose crests represent the main target for hydrocarbon exploration. The pattern of faults consists of two major sets of trends; the first pattern is longitudinal parallel to the axis of the rift created in an extensional regime during Neogene period. The second is transverse faults with N-S to NE-SW dominant trend which inherited passive discontinuities in the Precambrian basement rock (Colleta et al., 1988). Figure (2) shows the main surface geologic units and structure setting at Sinai Peninsula (Omara, 1972, and Kora, 1995).

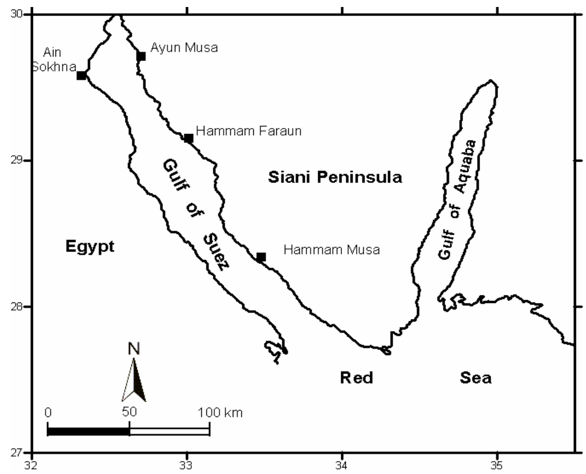

Figure 1: Location map of the hot springs on the eastern and western sides of the Gulf of Suez.

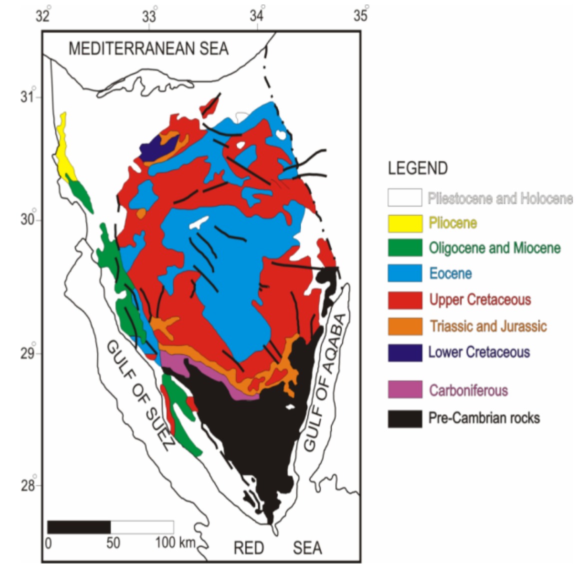

Figure 2: Main surface geology and structure setting of Sinai Peninsula.

3. GEOTHERMAL STUDIES

The mechanics of thermal process controlling the tectonic evolution of the Gulf of Suez is still abstruse. However, the anomalously large size of the rift flank for the amount of extension at the Gulf of Suez suggests components of uplift causing thermal expansion (Stickler, 1985; Feinstein et al., 1996). Geothermal studies were made based on bottom-hole temperature logs of 103 deep oil wells distributed in Gulf of Suez. These measurements were carried out by many oil companies such as Egyptian General Petroleum Company (EGPC), Gulf of Suez Petroleum Company (GUPCO) and British Petroleum Company (BPC). In order to avoid the affect of the variation of the logs depths, geothermal gradient was obtained collectively by grouping data from wells that are located close to one another and the mean of these grouping values is the characteristic temperature gradient value for the center hole (Fig. 3).

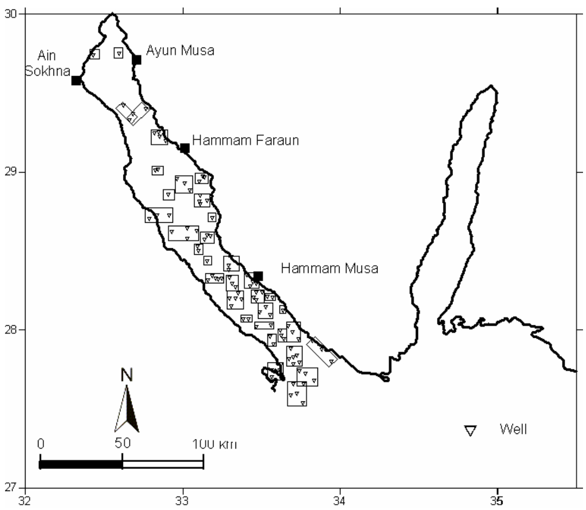

Figure 3: Locations of the oil wells used in geothermal studies, the geothermal gradient was obtained collectively by grouping data from wells that are located close to one another.

Temperature gradients were computed for the linear sections of the temperature-versus-depth plotted by least squares regression analysis and the main gradient at each well location was measured and listed taking the main surface temperature to be 26.7^{o}C. These temperature gradient determinations are shown in Table 1. High temperature gradient encountered around the hot springs manifestations and at the southern part of the Gulf of Suez, leading expectation of proving hot rock reserves at relatively shallow depths (Fig. 4). The maximum gradient was recorded near Hammam Faraun and Hammam Musa areas (0.06^{o}C/m); such gradient may be the highest recorded in geothermal exploration in whole Egypt.

Also, heat-flow values are determined by combining sets of temperature gradient and thermal conductivity data by the formula $Q = K(dt/dz)$, where Q is heat flow, K is thermal conductivity, and t is temperature at depth z. Simultaneously, the most suitable method for determining the heat flow is to divide the whole area into several sections and calculate the heat flow value in each section; the mean of these values is the characteristic heat flow value for the hole. Preliminary heat flow values ranging from 50 to 160 mWm-2 have been computed for Gulf of Suez with a reasonably good geographical distribution, and a limited number of thermal conductivity determinations (Fig. 5). The high heat flow and the sharp spatial variation both suggest the existence of a heat anomaly located at relatively shallow depths, probably due to the emplacement of plutonic bodies.

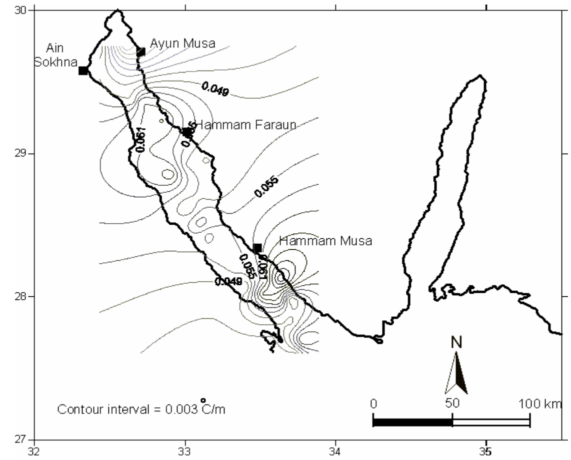

Figure 4: Temperature gradient map of the Gulf of Suez, high values are encountered around the hot springs manifestations on the eastern margin of the Gulf of Suez.

Table 1: Determined geothermal parameters including; temperature gradient and heat flow, which obtained collectively by grouping data from wells that are located close to one another and the mean of these grouping values is the characteristic value for the center hole.

Wells	Temperature gradients (^{o}mK/m)	Thermal conductivity (W/m_K)	Heat flow (mW/m^2)
1	0.0608	2.333	141.8
2	0.0487	2.8	136.4
3	0.0515	2.8	144.2
4	0.0495	2.566	127.1
5	0.0574	2.566	147.3
6	0.0576	2.166	124.8
7	0.0546	2.566	140.3
8	0.0535	2.6	139.2
9	0.0600	2.333	140.1
10	0.0629	2.633	165.7
11	0.0457	2.8	128.1
12	0.0577	2.6	150.02
13	0.0644	2.6	167.44
14	0.0512	2.75	141.0
15	0.0489	2.675	130.9
16	0.0567	2.275	129.1
17	0.0569	2.575	146.5
18	0.0463	2.7	125.1
19	0.0653	2.825	184.6
20	0.0535	2.6	139.1
21	0.0538	2.5	134.5
22	0.0454	2.9	131.8
23	0.0481	2.9	139.5
24	0.0598	2.6	155.4
25	0.0601	2.4	144.2
26	0.0663	2.4	159.1
27	0.0587	2.9	170.2
28	0.0678	2.3	156.0
29	0.0459	2.35	107.9
30	0.0509	1.8	91.6
31	0.0518	2.6	134.6
32	0.0793	2.1	166.5
33	0.0663	2.6	172.3
34	0.0502	2.9	145.5
35	0.0252	2	50.4

4. GEOPHYSICAL STUDIES

4.1 Aeromagnetic Map

In the present work, the total intensity magnetic map of the Gulf of Suez is reduced to the pole based on Cochran et al. (1986), and Meshref (1990)

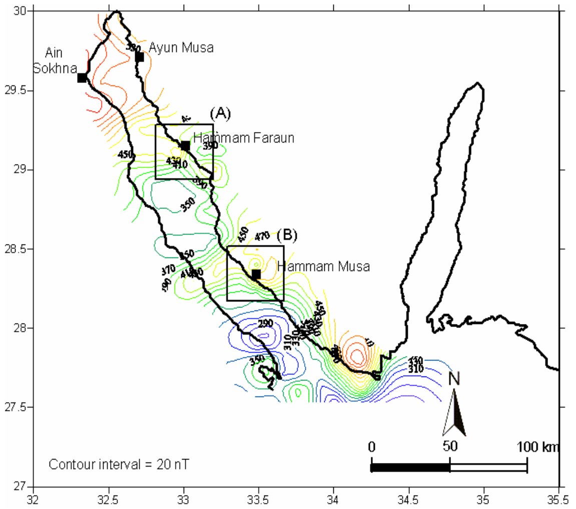

Figure 5: Heat flow map of the Gulf of Suez measured by combining sets of temperature gradient and thermal-conductivity data.

Magnetic anomalies are range between 250–600 nT. Positive anomalies are thought to correspond to the location of the uplift of the basement rocks on the eastern and western side of the Gulf of Suez. The quantitative use of aeromagnetic surveys is to determine basement depth depending on the nature of the magnetic disturbances produced by magnetized bodies of various geometric forms (Fig. 6).

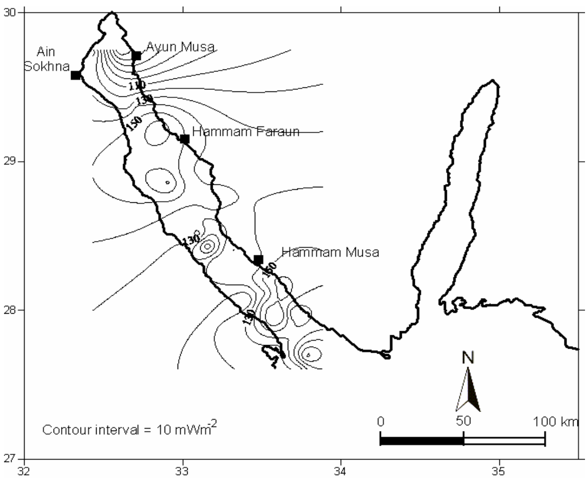

Figure 6: Total intensity magnetic map of the Gulf of Suez, reduced to the pole, shows positive anomalies above hot springs areas (A and B).

The fast Fourier transform, used to convert the space domain grid data to the Fourier domain, was applied on the magnetic data for calculating the energy spectrum curve and estimating the depths of shallow and deep magnetic sources on both Hammam Faraun and Hammam Musa hot springs areas. A technique was applied on the aeromagnetic map including the estimation of analytical signal of the magnetic anomalies. This can be easy calculated from the three orthogonal gradients of the total magnetic field (Roest et al. 1992) by using the following expression.

$$\left|A_T(x,y)\right| = \sqrt{\left(\frac{\partial T}{\partial x}\right)^2 + \left(\frac{\partial T}{\partial y}\right)^2 + \left(\frac{\partial T}{\partial z}\right)^2} \qquad (1)$$

where $\left|A_T(x,y)\right|$ is the amplitude of the analytic signal at (x, y), T is the observed of total magnetic intensity at (x, y). The amplitude of the analytic signal of the total magnetic field produces maxima over magnetic contacts regardless of the direction of magnetization. The map of the analytic signal of the magnetic anomalies recorded the maxima above the two main hot springs in the eastern side of the Gulf of Suez, Hammam Faraun and Hammam Musa hot springs (Fig. 7).

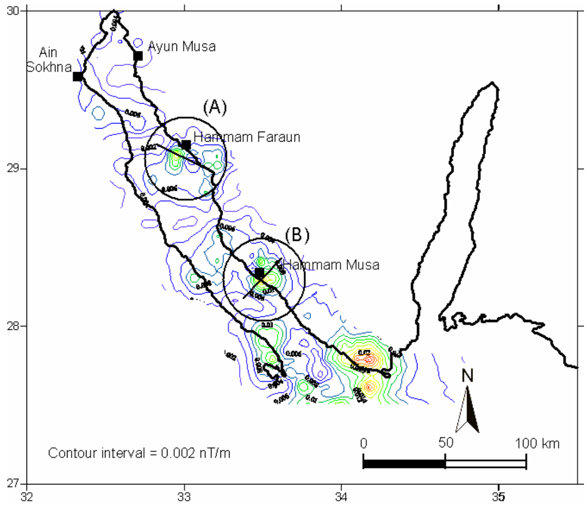

Figure 7: Analytical signal map of the magnetic anomalies on the Gulf of Suez calculated from the three orthogonal gradients of the total magnetic field.

Nabighian (1972) made expression which describes the analytic signal over a 2-D magnetic anomaly located at (x=0) and at depth h:

$$\left|A(x)\right| = \alpha \frac{1}{(h^2+x^2)^{1/2}} \qquad (2)$$

Where A(x) is the analytic signal and α is the amplitude factor. The depth to the magnetic sources can be derived from the analytic signal anomaly width at half of the amplitude (Atchuta et al, 1981 and Roest et al,1992) directly from equation 2.

$$x_{1/2} = 2\sqrt{3}h = 3.46h \qquad (3)$$

where the $x_{1/2}$ is the width of the anomaly at half of the amplitude and h is the depth to the top of the source. The result from the analytic signal of the magnetic anomaly over Hammam Faraun and Hammam Musa shows the depth to the upper surface of the magnetic contact to be 1.7 and 3.2 respectively (Fig. 8).

4.2 Bouguer Anomaly Map

The present geophysical study depends on the Bouguer anomaly map of the Gulf of Suez Scale 1:500,000 published by the General Petroleum Company (GPC), 1980 (Fig. 9). The gravity values of the Gulf of Suez range from -10 mgal to -50 mgal. The most significant features in the Bouguer anomaly map are the steep gradients from high to low gravity values on the edges of the Gulf and especially above the hot springs which can be interpreted as being associated with large normal and strike slip faults that control the geometry of the Gulf of Suez. Gravity highs are in many areas associated with anticlines or uplifted blocks, with older denser rocks becoming nearer to the surface. Conversely, sedimentary basins which have thicker sediments usually produce gravity lows. The belts of marked gradient are produced by steep contact between different rock types, which mainly occur across fault planes. The geothermal areas are marked by a positive gravity anomaly which may be caused by uplift of high dense basement rocks; however, the large scale of the Bouguer anomaly map hindered a closer structural investigation of the anomaly.

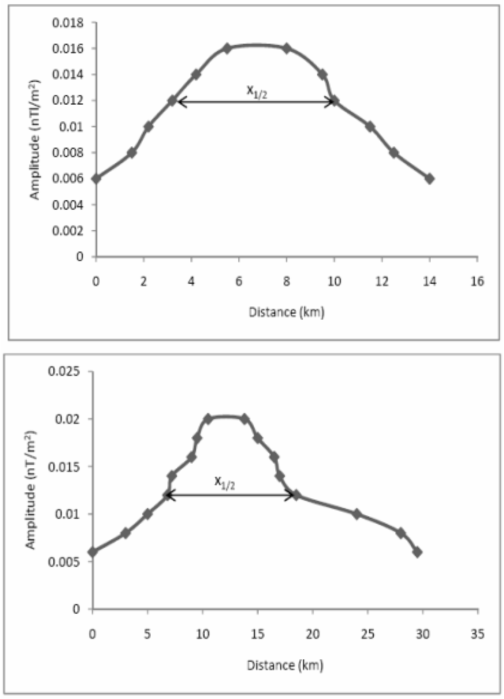

Figure 8: Amplitudes of the analytic signals of profiles A and B, the depth to the magnetic sources were estimated from the analytic signal anomaly width at half the amplitude.

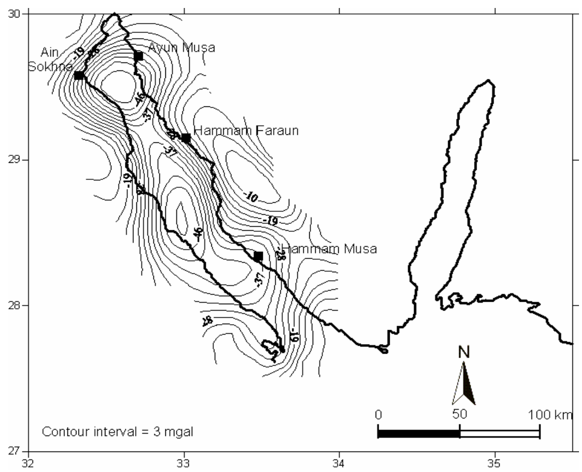

Figure 9: Bouguer anomaly map of the Gulf of Suez Scale 1:500,000 published by the General Petroleum Company (GPC).

Horizontal gradient technique of the Bouguer anomaly map of the Gulf of Suez is calculated as the Pythagorean sum of the gradients in the orthogonal directions.

$$H.G = \sqrt{\left(\frac{\partial T}{\partial x}\right)^2 + \left(\frac{\partial T}{\partial y}\right)^2} \quad (4)$$

The horizontal gradient (HG) method is considered as the simplest approach to estimate the contact locations such as faults where the maximum horizontal gradient (more properly the maxima of the total horizontal gradient) of the anomaly slope is located near or over the body edge. That is, the horizontal gradient operator in map form produces maximum ridges over edges of high dense basement blocks and faults or other dense bodies. In addition, the horizontal gradient highlights linear features, related to contacts, in the data set. The geothermal areas in the eastern costs as well as the southern part of the Gulf of Suez are associated with maximum values of horizontal gradient on the Bouguer anomaly map which may elucidate the origin of these geothermal resources Fig. (10).

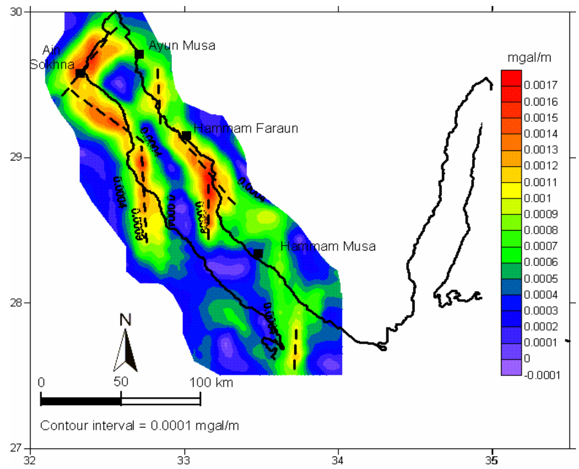

Figure 10: Horizontal gradient map of the Bouguer anomalies of the Gulf of Suez calculated as the Pythagorean sum of the gradients in the orthogonal directions.

CONCLUSION

Bottom-hole temperature (BHT) data are collected from “deep” wells in sedimentary basins from oil wells data as a source of subsurface temperature information in order to evaluate potential geothermal resources in Gulf of Suez region.

Temperature gradients map on the Gulf of Suez shows highest gradient southward and on rift margins and horst blocks in the Gulf of Suez. Simultaneously, High heat flows are recorded at the edges of the Gulf of Suez and on the hot springs regions and the maximum record was 160 mWm-2 around Hammam Faraun hot spring. Geophysical studies on Gulf of Suez including gravity and magnetic techniques show a good coherence between high heat flow areas and gravity and magnetic anomalies. Thus, the thermal maturity lines on any cross section across the Gulf of Suez would be slightly concave and reflective of basement structure. Horizontal gradient of the Bouguer anomaly map shows the maxima on the eastern Gulf margin as well as hot spring regions on the eastern and western sides which reflect that these geothermal manifestations associating with vertical faults may be associated with the Red Sea and Gulf of Suez opening. The map of the analytic signal of the magnetic anomalies showed the maxima above the two main hot springs in the eastern side of the Gulf of Suez, Hammam Faraun and Hammam Musa hot springs. The depth to the geothermal sources determined from the geophysical processing recorded to be 1.7 km and 3.2 km at Hammam Faraun and Hammam Musa areas, respectively.

ACKNOWLEDGMENT

The authors are grateful to Egyptian General Petroleum Company (EGPC), Gulf of Suez Petroleum Company (GUPCO) and British Petroleum Company (BPC) for their assistance to collect temperature wells on Gulf of Suez region.

REFERENCE

Abdel Gawad, M., The Gulf of Suez: A brief review of stratigraphy and structure. Phil. Trans. Roy. Soc. London. A.267, 41-48 (1970).

Atchuta Rao, D., Ram Babu, H. V., and Sanker Narayan, P. V., Interpretation of magnetic anomalies due to dikes: The complex gradient method: Geophysics, 46, 1572-1578 (1981).

Cochran, J.R., Martinez, F., Steckler, M.S., Hobart, M.A., Conrad deep: a new northern Red Sea deep. Origin and implications of continental rifting. Earth. Planet Sci. Lett. 78, 18–32 (1986).

Colletta, B., P. Le Quellec, J. Letouzey, and I. Moretti, Longitudinal evolution of the Suez rift structure (Egypt), Tectonophysics, 153, 221–233 (1988).

Feinstein, S., Kohn, B., Steckler M., and Eyal, M., Thermal history of the eastern margin of the Gulf of Suez, I. Reconstructed from borehole temperature and organic maturity measurements. Tectonophysics, 266, 203-220 (1996).

Fournier, R.O., Potter, R.W., “Magnesium correction to Na-K-Ca chemical geothermometer”, Geochim. Cosmochim. Acta 43, 1543–1550 (1979).

Fournier, R. O. and Truesdell, A. H.,. An empirical Na-K-Ca geothermometer for natural waters. Geochim. Cosmochim. Acta, 37: 1255-1275 (1973)

General Petroleum Corporation, A.S.R.T., Bouguer gravity map of Egypt. Scale 1:500,000 (1980).

Giggenbach, W. F., 1988. Geothermal solute equilibria. Derivation of Na-K-Ca-Mg geoindicators. Geochim. Cosmochim. Acta, 52: 2749-2765.

Kora, M., An introduction to the stratigraphy of Egypt. Lecture notes, Geology Dept. Mansoura Univ., 116pp (1995)

McKenzie D. P., Davies D., Molnar P., Plate Tectonics of the Red Sea and East Africa. Nature 226, 243–248 (1970).

Meneisy, M.Y., Volcanicity, Chapt.9, In Said, R.(Ed.) Geology of Egypt, Balkema Pub. Rotterdam, Netherlands, 157-172 (1990).

Meshref, W.M., Tectonic framework. In: Said, R. (Ed.), The Geology of Egypt. A.A. Balkema, Rotterdam, pp. 113–155 (1990).

Nabighian, M.N., The analytic signal of two-dimensional magnetic bodies with polygonal cross-section: Its properties and use for automated anomaly interpretation: Geophysics, 37 507-517 (1972).

Nieva and Nieva, 1987 D. Nieva and R. Nieva, Developments in geothermal energy in Mexico. Part twelve: a cationic geothermometer for prospecting of geothermal resources, Heat Recov. Syst. 7, pp. 243–258 (1987).

Omara, S., An early Cambrian outcrop in southwestern Sinai, Egypt. N.JP. Geol.Palaeontol. 5, 306-314 (1972).

Roest, W.E., Verhoef, J., Pilkington, M., Magnetic interpretation using 3-D analytic signal: Geophysics, 57, 116-125 (1992).

Said, R., The Geology of Egypt. Elsevier, Amstredam, 377 pp (1962).

Steckler, M., Uplift and extension at the Gulf of Suez-indication of induced mantle convection. Nature, 317, 135-139 (1985).

United States Geological Survey (USGS), The Red Sea Basin Province, Open –File Report 99-50-A (1998).

Verma, M.P., Revised quartz solubility temperature dependence equation along the water-vapor saturation curve, in World Geothermal Congress, Kyushu-Tohoku, Japan, 1927-1932 (2000).